Higgs boson measurements in its decays into bosons with the ATLAS experiment

UMassAmherst

Rafael Coelho Lopes de Sá
On behalf of the ATLAS collaboration
University of Massachusetts Amherst

ATLAS EXPERIMENT

The XXVIII International Conference on Supersymmetry and Unification of Fundamental Interactions

August 26th, 2021

Introduction

- Higgs decays to gauge bosons provide precise probes of the Higgs boson properties
- This talk reviews recent results from the ATLAS collaboration in the $H \to WW$, $H \to \gamma\gamma$, and $H \to ZZ$ decay channels.
- The large integrated luminosity collected during the Run 2 of the LHC allows for a large number of measurements to be performed, providing detailed information about the Higgs boson.
- Simplified Template Cross Section (STXS) measurements and Effective Field Theory (EFT) searches are examples of measurements that are becoming more powerful with the full Run 2 dataset.
- The results that will be presented here are:
  - $H \to WW$ production in ggF and VBF, including STXS measurements
  - $H \to \gamma\gamma$ production, including STXS measurements
  - $H \to ZZ$ production, including differential cross-sections, STXS, and EFT measurements

Simplified Template Cross Section (STXS) Measurements

- Measure Higgs production modes separately. Within each production mode, regions are defined based on relevant variables for theoretical calculations and for BSM physics ($p_T^H, N_{\text{jets}}, m_{jj}, p_T^V, p_T^{Hjj}, \ldots$).
- Since regions are not defined by final-state particles (like in fiducial cross sections), different decay modes of the Higgs boson can be easily combined.
- Framework provided in stages (0, 1, 1.1, 1.2, …) with different granularity. Level of granularity to be used based on the amount of data available [more details].

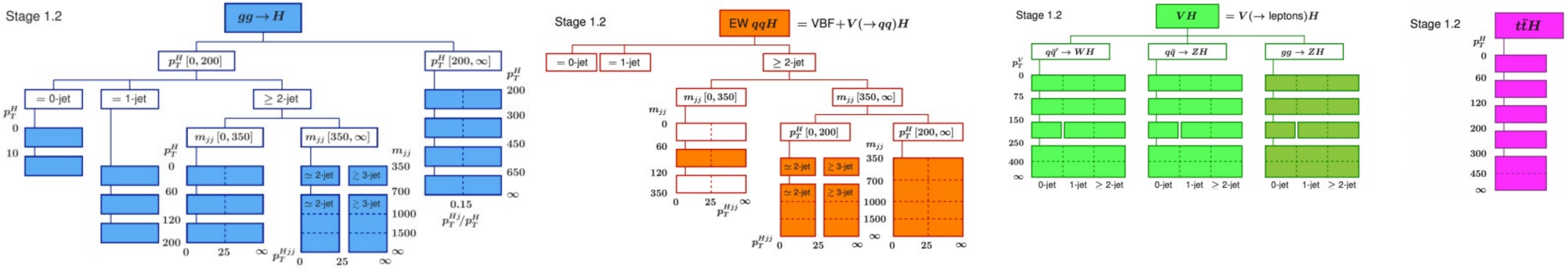

Experimental challenge: define large number of analysis regions to maximize sensitivity.

Rafael Coelho Lopes de Sá

Simplified Template Cross Section (STXS) Measurements

ATLAS EXPERIMENT

UMassAmherst

- Measure Higgs production modes separately. Within each production mode, regions are defined based on relevant variables for theoretical calculations and for BSM physics ($p_T^H, N_{\text{jets}}, m_{jj}, p_T^V, p_T^{Hjj}, \ldots$).
- Since regions are not defined by final-state particles (like in fiducial cross sections), different decay modes of the Higgs boson can be easily combined.
- Framework provided in stages (0, 1, 1.1, 1.2, …) with different granularity. Level of granularity to be used based on the amount of data available [more details].

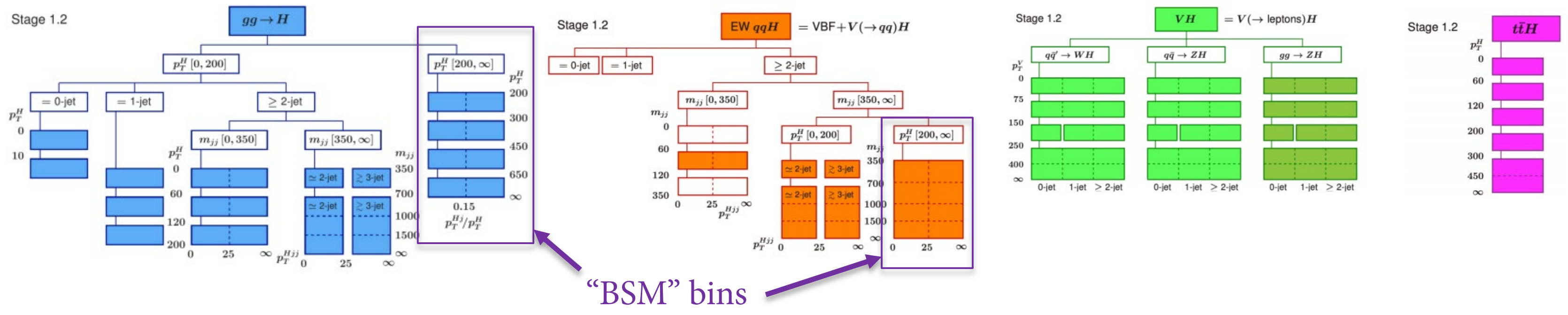

Experimental challenge: define large number of analysis regions to maximize sensitivity.

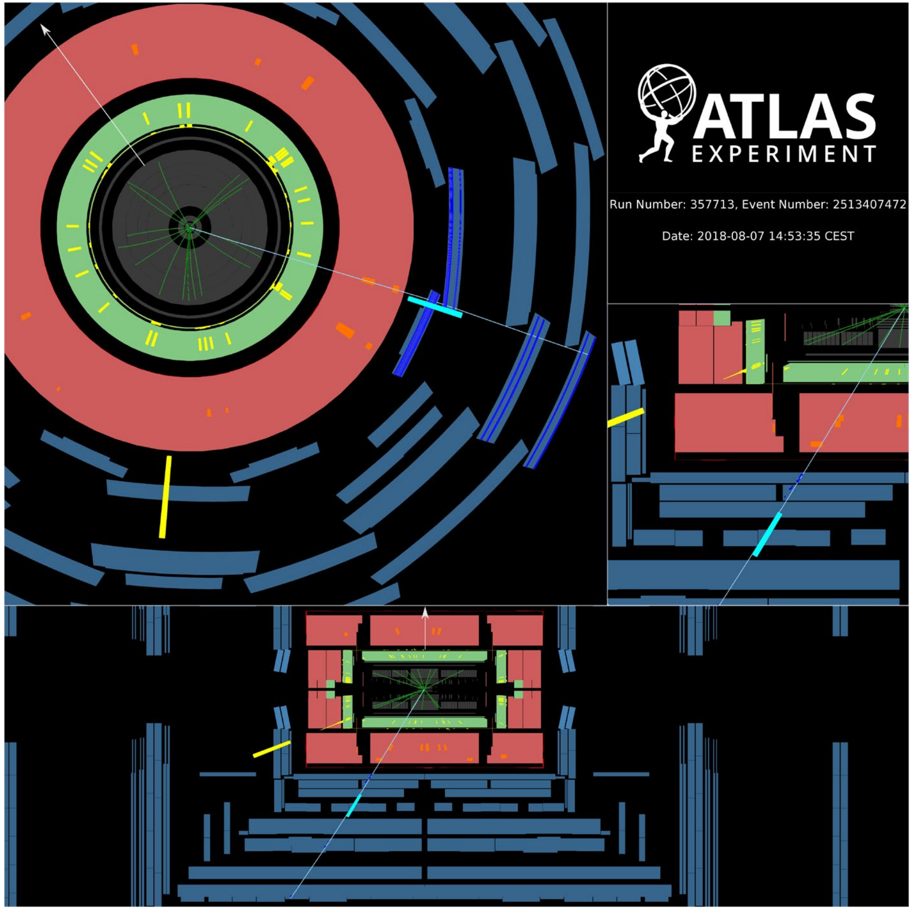

$H \rightarrow WW$ results

ATLAS-CONF-2021-014

$H \rightarrow WW$ measurement

- Measurement in the $H \rightarrow WW \rightarrow e\nu\mu\nu$ final state
- Analysis performed in N_{jets} regions to increase sensitivity to different production modes (ggF, VBF)
- Channel with $N_{\text{jets}} \geq 2$ uses dedicated DNN to identify the VBF topology.
- For channels targeting ggF production, the transverse mass $m_T^{\ell\ell}$ is used as discriminating variable.

- Large background from non-resonant WW and $t\bar{t}$ processes.
- Background processes normalized in dedicated data control regions.

N_{jets} after preselection

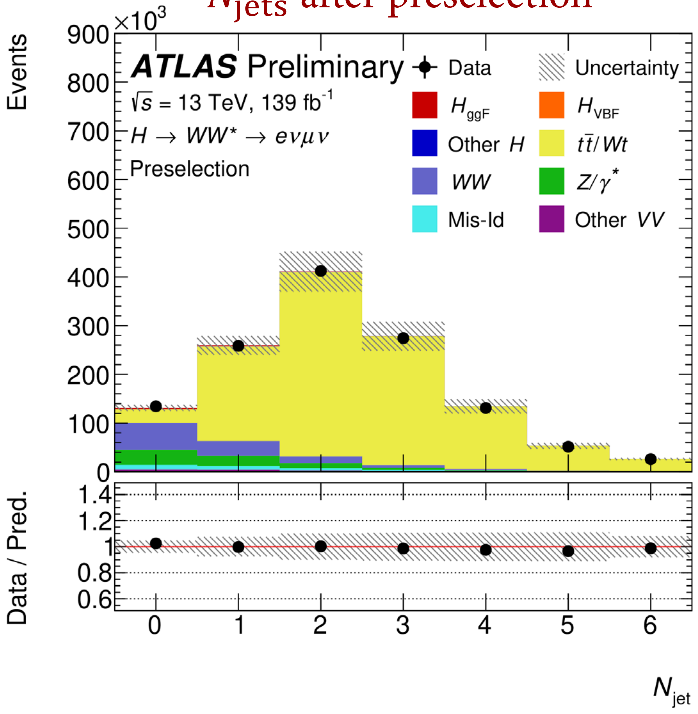

$H \to WW$ strategy

- Different analysis strategy are used for different N_{jets} channels. All channels with b-jet veto to reduce $t\bar{t}$.
- $N_{\text{jets}} = 0$
  - Reduce background requiring $\Delta\phi_{\ell\ell,E_T^{\text{miss}}} > \frac{\pi}{2}$, $p_T^{\ell\ell} >$ 30 GeV, $m_{\ell\ell} <$ 55 GeV and $\Delta\phi_{\ell\ell} < 1.8$
  - Binned in $(m_T^{\ell\ell}, m_{\ell\ell}, p_T^{\text{sublead } \ell})$
- $N_{\text{jets}} = 1$
  - Same $m_{\ell\ell}$ and $\Delta\phi_{\ell\ell}$ selection as above
  - $m_{\tau\tau} < m_Z - 25\ GeV$, $\max(m_T^{\ell}) >$ 50 GeV
  - Binned in $(m_T^{\ell\ell}, m_{\ell\ell}, p_T^{\text{sublead } \ell})$
- $N_{\text{jets}} \geq 2$ VBF
  - Central jet veto, outside lepton veto, $m_{jj} >$ 120 GeV
  - Binned in DNN

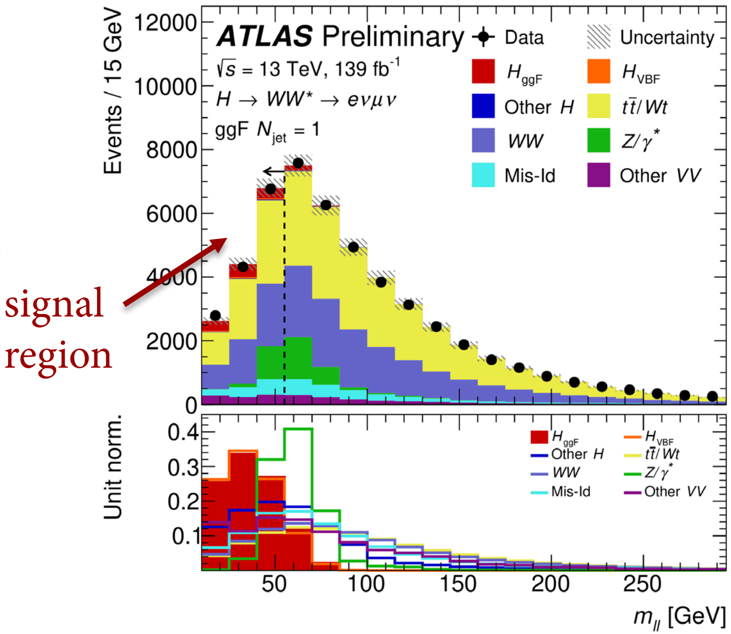

- $N_{\text{jets}} \geq 2$ ggF
  - Fails VBF selection, $|m_{jj} - 85| >$ 15 GeV, $\Delta y_{jj} > 1.2$
  - Binned in $(m_T^{\ell\ell}, m_{\ell\ell})$

$H \rightarrow WW$ results

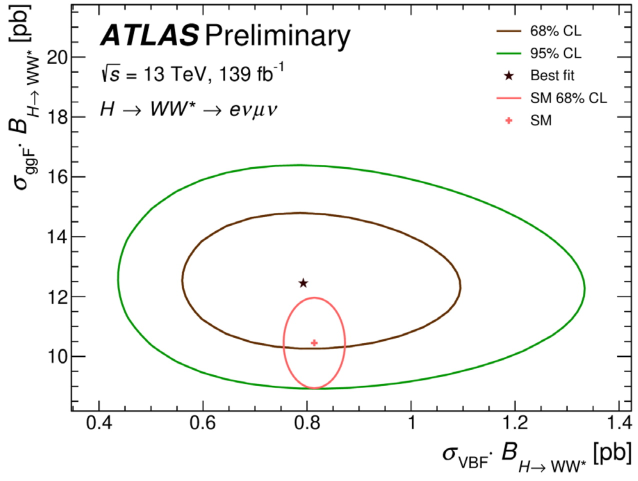

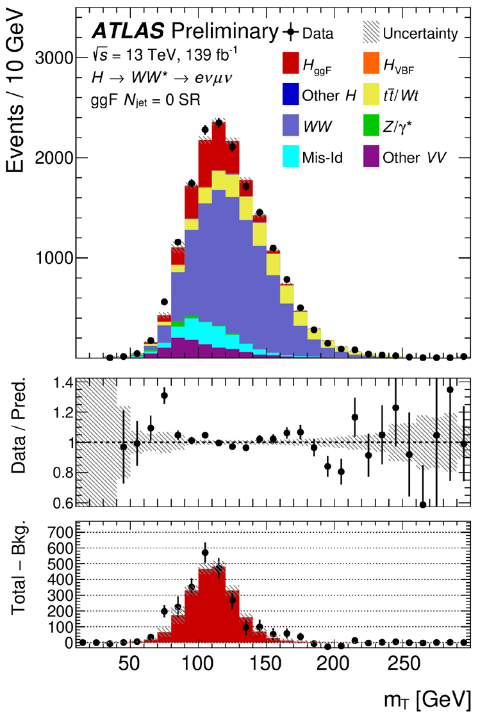

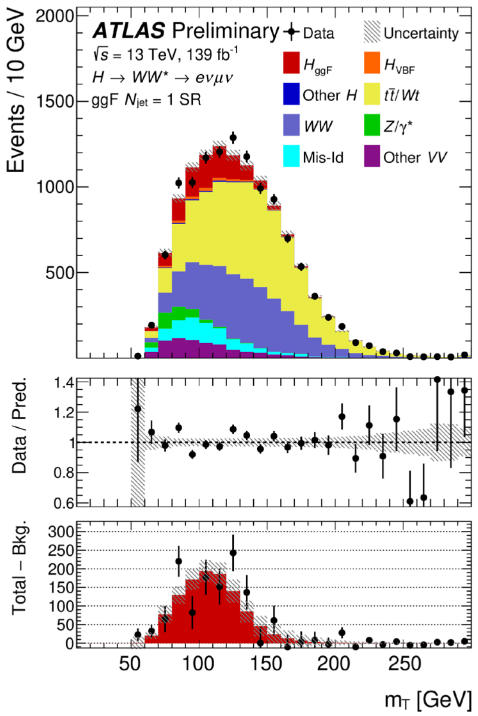

$H \to WW$ results

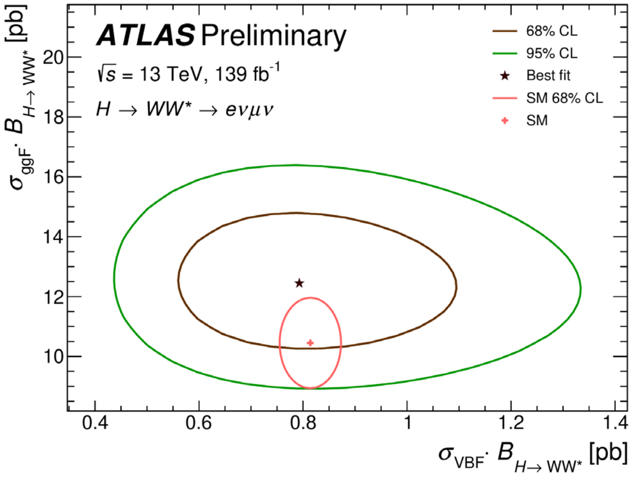

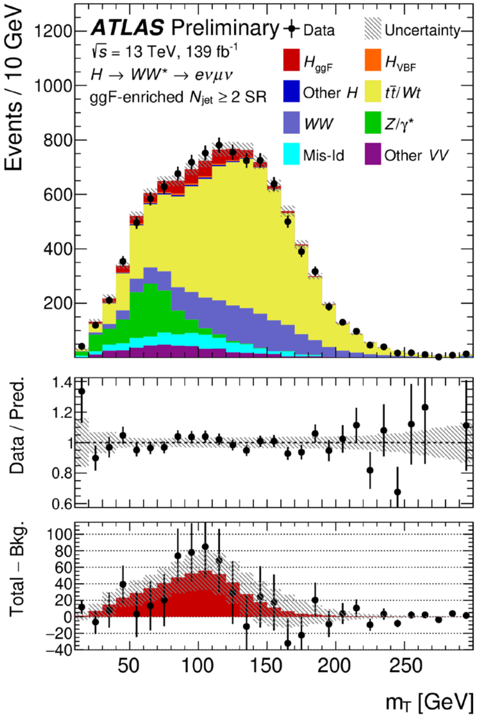

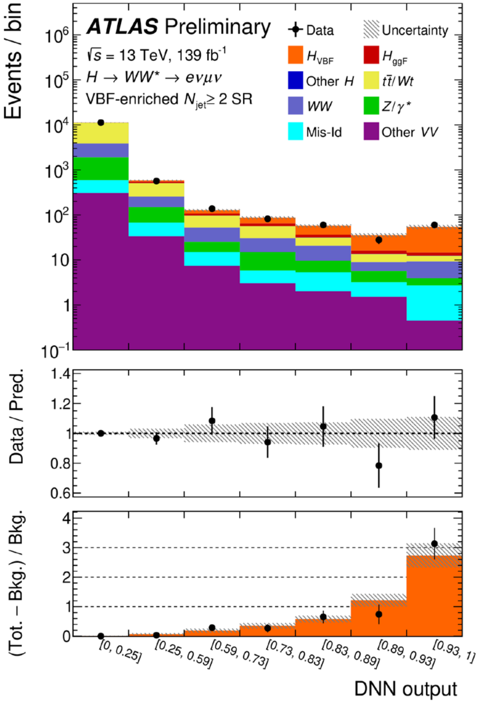

ATLAS EXPERIMENT

UMassAmherst

$H \rightarrow WW$ STXS interpretation

- The measurement is interpreted in a "reduced" Stage-1.2 STXS framework.
- STXS parameters are merged in the following categories:
  - $N_{\text{jets}} = 0$ ggH category, $p_T^H < 200$ GeV
  - $N_{\text{jets}} \geq 2$ ggH category, $p_T^H < 200$ GeV
  - N_{jets} inclusive ggH category, $p_T^H > 200$ GeV
  - $N_{\text{jets}} \geq 2$ EW qqH category, bins in p_T^{Hjj} are merged. Bins in m_{jj} are reduced to only 5.
- Similar selections are applied in the analysis when performing the STXS interpretation.

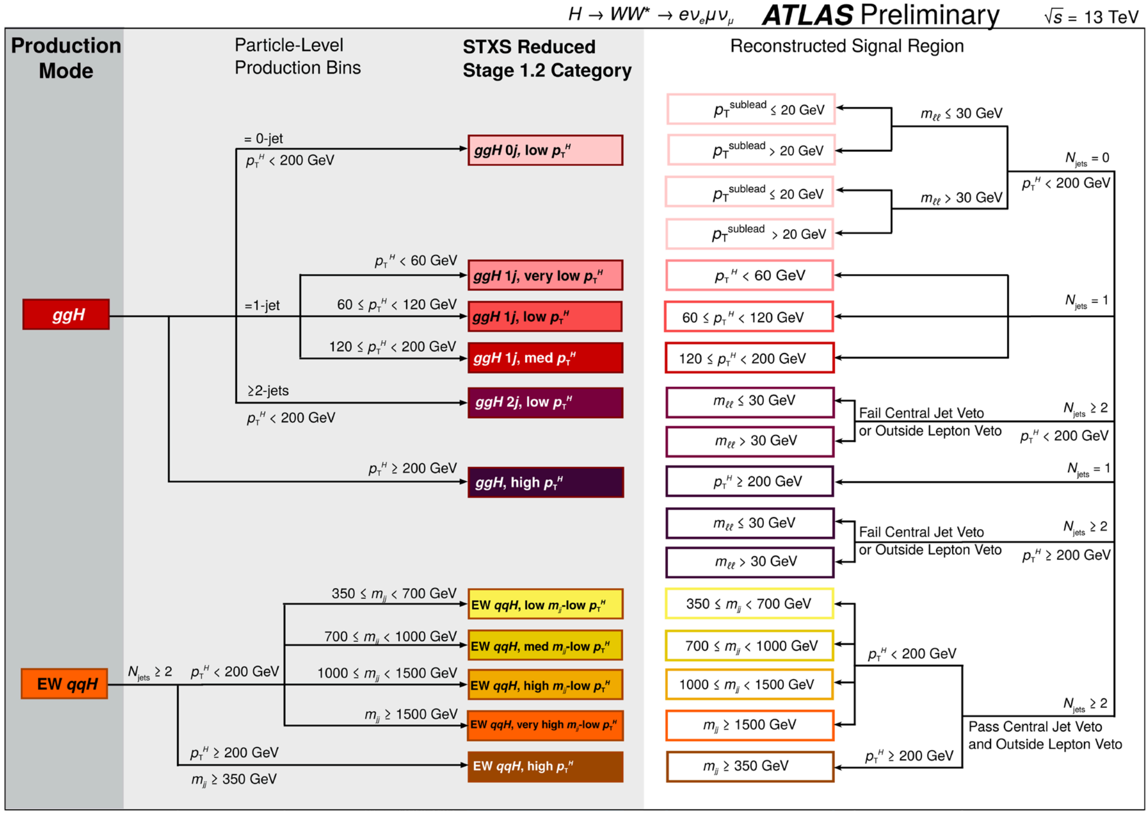

$H \to WW$ STXS interpretation

- The measurement is interpreted in a "reduced" Stage-1.2 STXS framework.
- STXS parameters are merged in the following categories:
  - $N_{\text{jets}} = 0$ ggH category, $p_T^H < 200$ GeV
  - $N_{\text{jets}} \geq 2$ ggH category, $p_T^H < 200$ GeV
  - N_{jets} inclusive ggH category, $p_T^H > 200$ GeV
  - $N_{\text{jets}} \geq 2$ EW qqH category, bins in p_T^{Hjj} are merged. Bins in m_{jj} are reduced to only 5.
- Similar selections are applied in the analysis when performing the STXS interpretation.

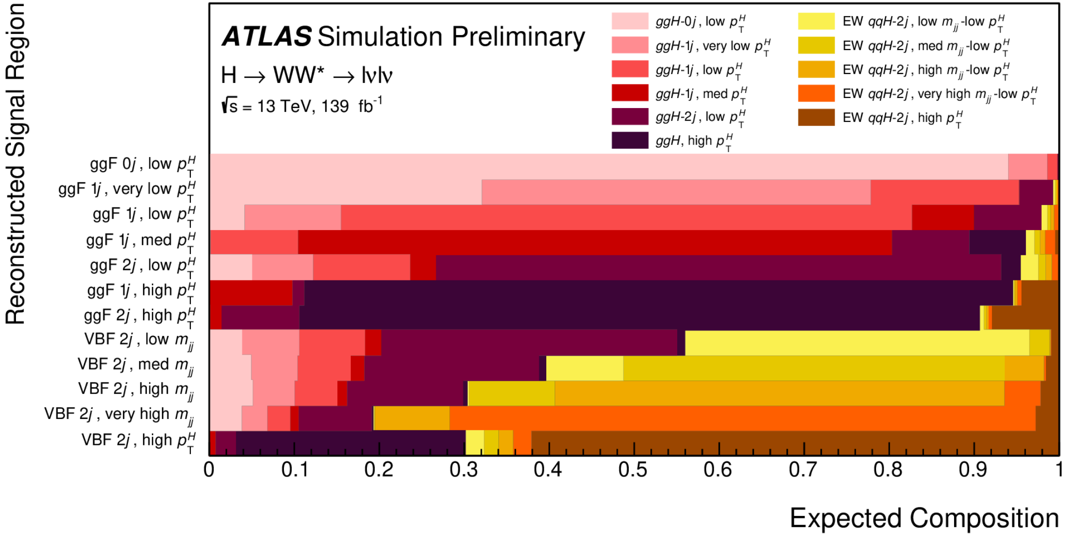

$H \to WW$ STXS results

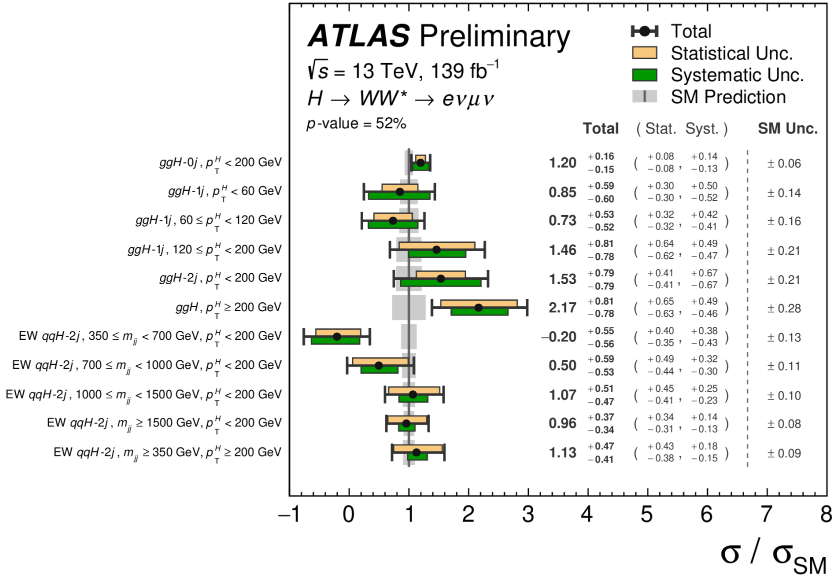

- Full run 2 measurement of the $H \to WW$ cross section in both ggF and VBF production modes
- The ggF cross section times branching ratio is measured:

$$12.4 \pm 0.6(\text{stat}) \pm 0.9(\text{exp syst})^{+0.7}_{-0.6}(\text{sig theo}) \pm 1.0(\text{bkg theo})\ \text{pb}$$

in good agreement with the SM prediction of 10.4 ± 0.6 pb

- The VBF cross section times branching ratio is measured:

$$0.79\ ^{+0.11}_{-0.10}(\text{stat})\ ^{+0.06}_{-0.05}(\text{exp syst})\ ^{+0.13}_{-0.09}(\text{sig theo})\ ^{+0.08}_{-0.06}(\text{bkg theo})\ \text{pb}$$

in good agreement with the SM prediction of 0.81 ± 0.02 pb

- The $H \to WW$ decay channel is further characterized in 11 STXS categories, which are compatible with the SM predictions with a p-value of 52%.

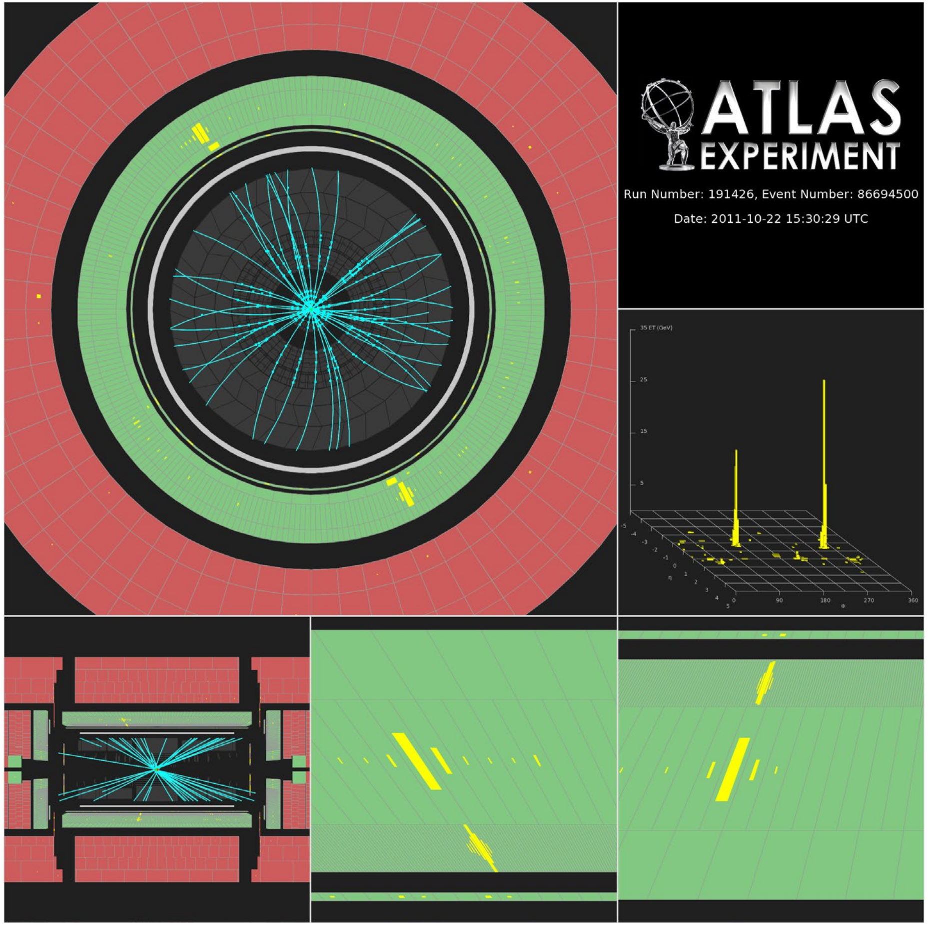

$H \rightarrow \gamma\gamma$ results

ATLAS-CONF-2020-026

$H \to \gamma\gamma$ analysis strategy

- Basic strategy of the analysis follows traditional $H \to \gamma\gamma$ analyses:
  - Select two tight photons
  - Dedicated NN for vertex reconstruction
  - Require $\frac{p_T^\gamma}{m_{\gamma\gamma}} > 0.35\ (0.25)$ for leading (subleading) photon.
- A large multi-class BDT is trained to classify events following the Stage 1.2 STXS definitions with few modifications:
  - $b\bar{b}H$ and $gg \to H$ processes are considered together.
  - $gg \to ZH$ and $q\bar{q} \to ZH$ processes are consider together.
  - The $p_T^H > 200$ GeV in the $qq' \to Hqq'$ category is split into $350 < m_{jj} < 700$ GeV and $m_{jj} > 700$ GeV regions.
- Events are selected based on the value of the multiclass BDT but also on the correlation between different channels in order to maximize total amount of information.

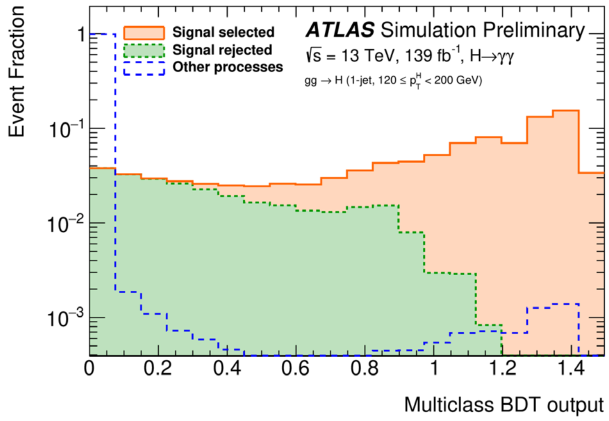

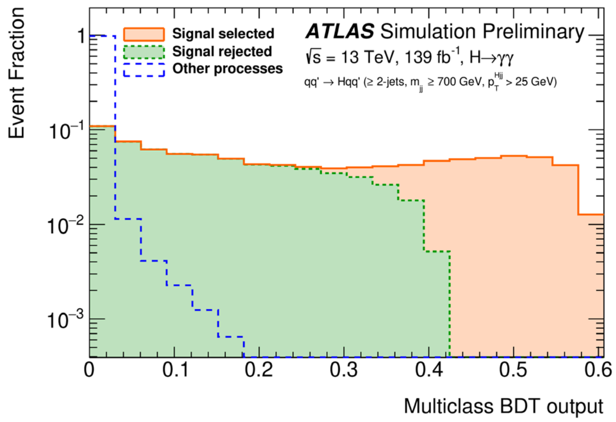

$H \to \gamma\gamma$ STXS regions

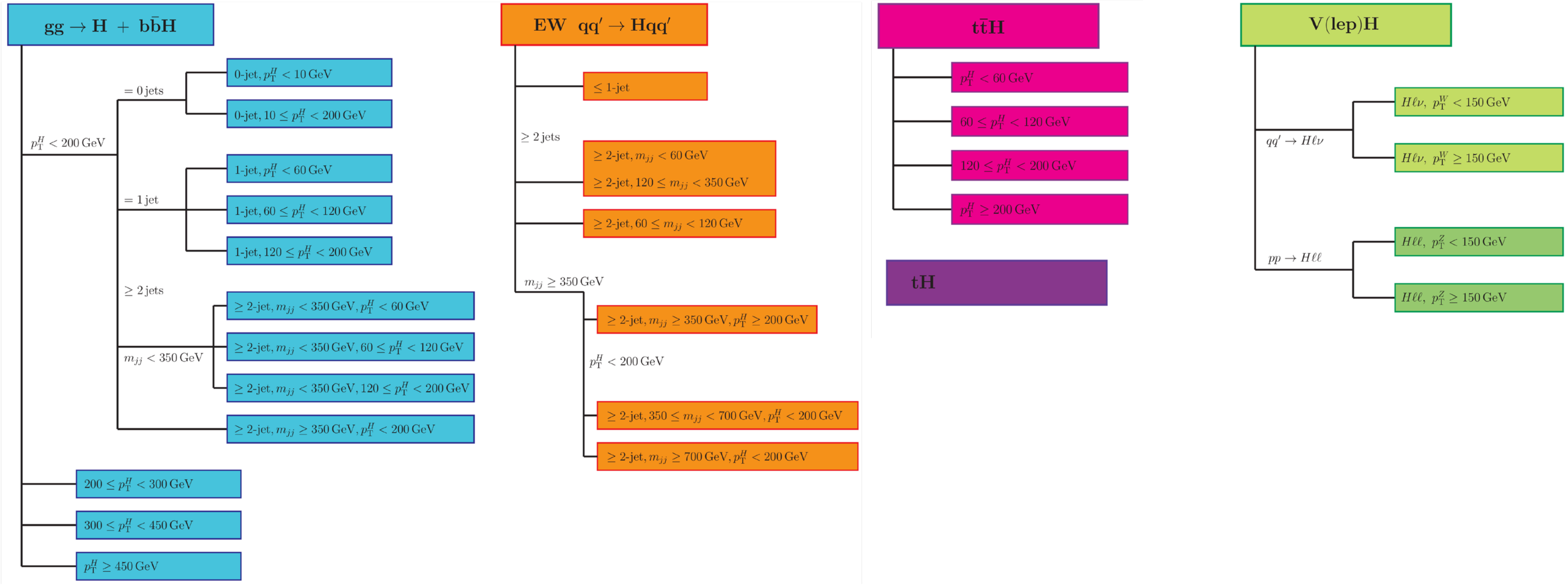

$H \rightarrow \gamma\gamma$ signal and background

- In order to further reject background from γj, jj, and from different STXS region, a binary BDT is trained in each region selected by the multiclass BDT.
- Selection using each BDT is chosen to maximize the significance of the channel.
- The PDF for the signal in each STXS is modeled as a double Crystal Ball density obtained from simulation.
- The PDF for the background is chosen from a number of candidate functions that are tested in a combination of data sidebands and simulated samples.
  - Disagreement in sidebands and MC sample can generate spurious signal.
  - Dominant source of systematic uncertainty in several STXS bins.

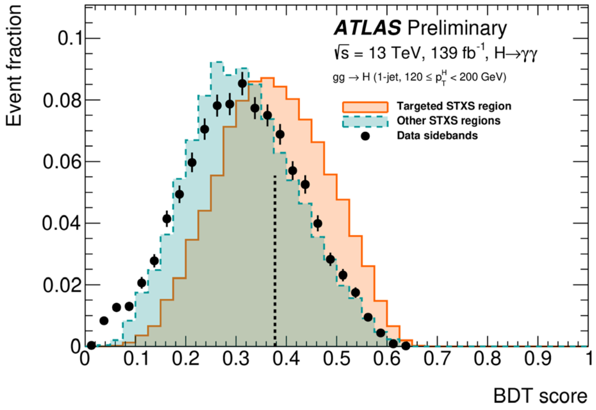

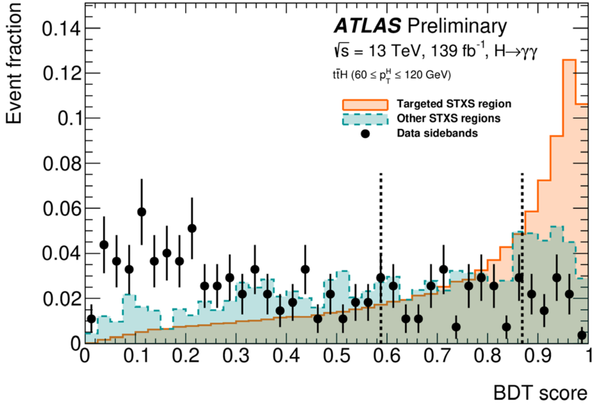

$H \to \gamma\gamma$ signal and background

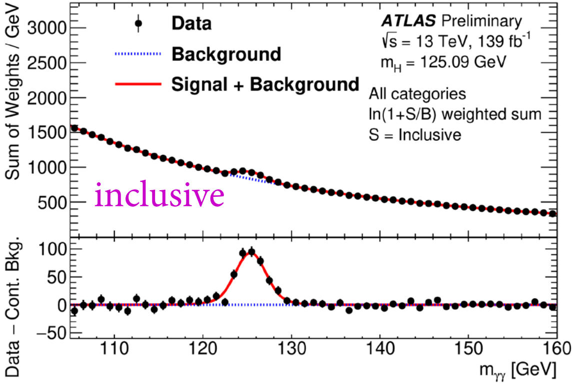

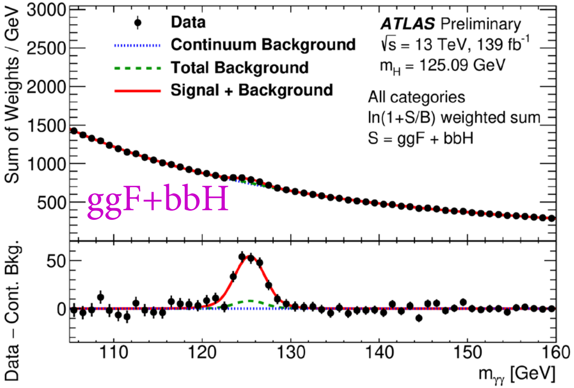

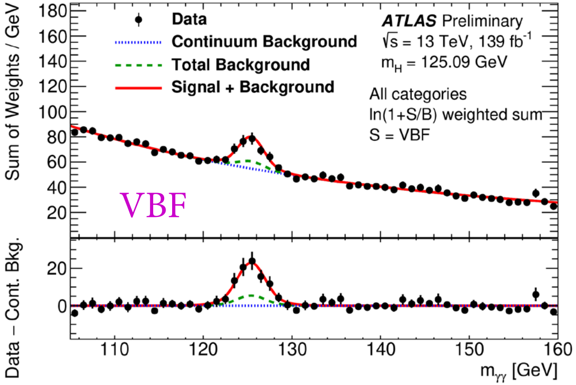

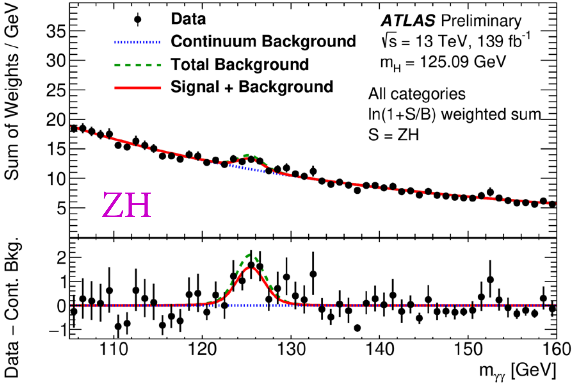

Rafael Coelho Lopes de Sá

UMassAmherst

$H \rightarrow \gamma\gamma$ results

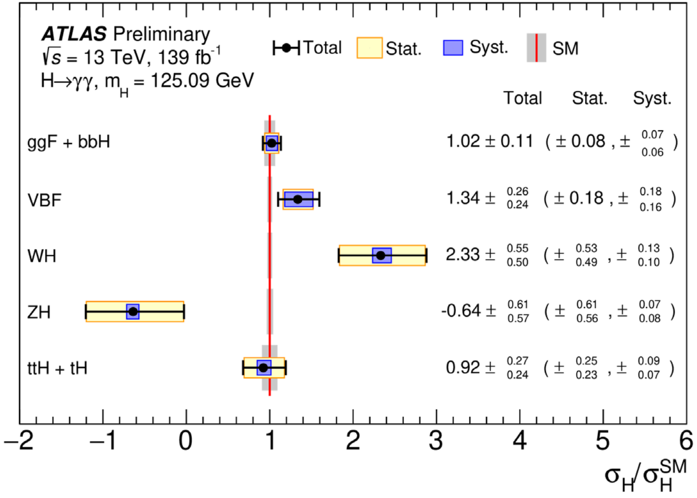

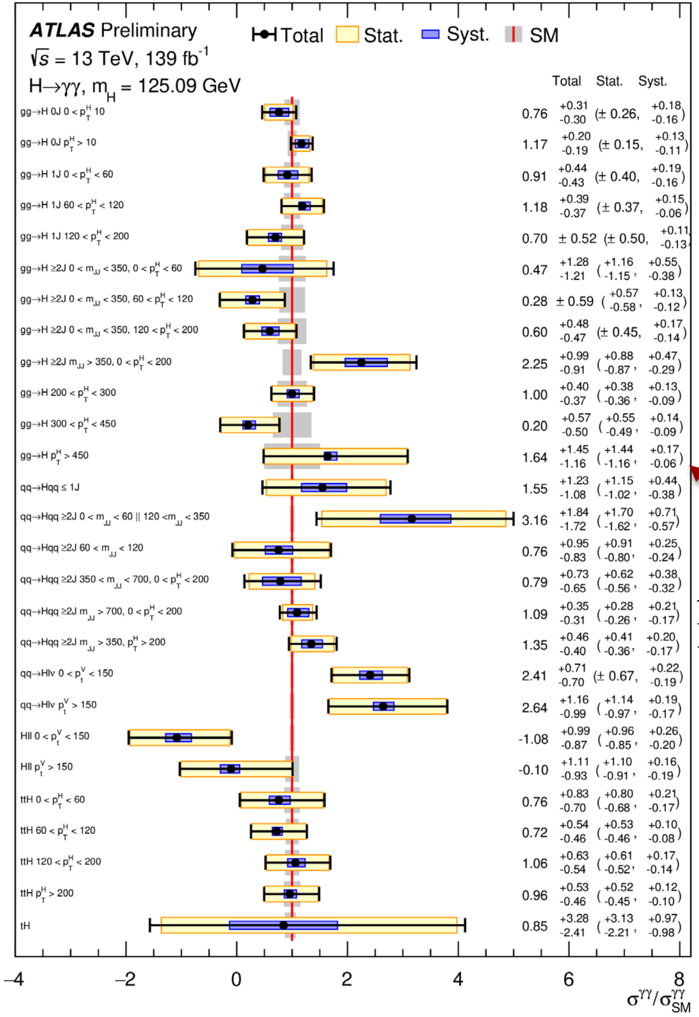

Access to very high Higgs $p_T^H > 450$ GeV !!!

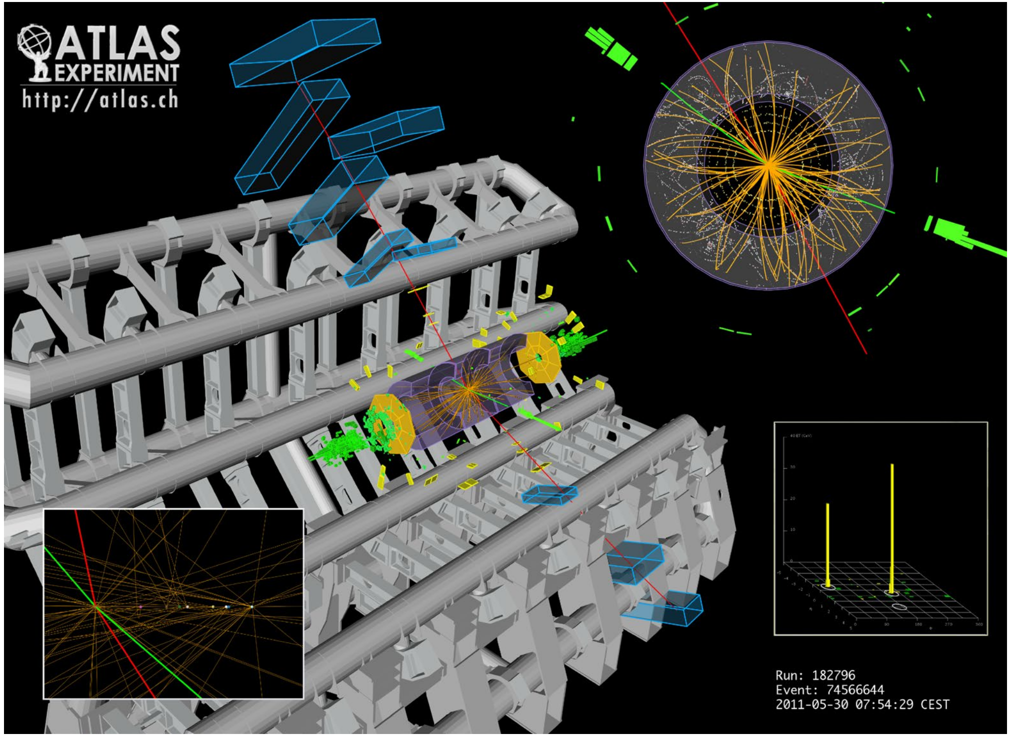

$H \rightarrow ZZ$ results

Eur. Phys. J. C 80 (2020) 942
Eur. Phys. J. C 80 (2020) 957

$H \rightarrow ZZ$ fiducial and differential cross section

- The channel $H \rightarrow ZZ \rightarrow 2\ell 2\ell'$ provides a very clean, yet low statistics channel to probe Higgs cross sections
- The large number of events collected during the Run 2 of the LHC allows for precision measurement of fiducial cross sections and for a large variety of differential cross sections.

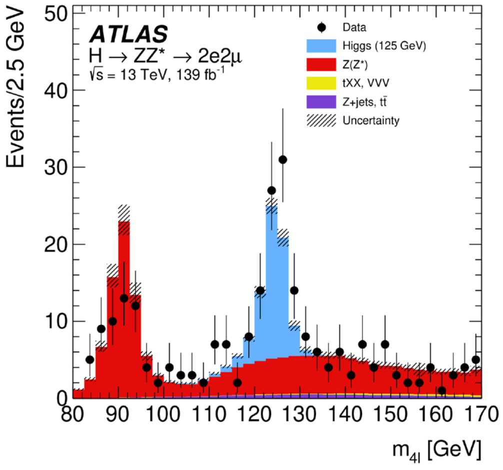

Fiducial region used in the measurement.

Leptons and jets	
Leptons	$p_T > 5$ GeV, $\|\eta\| < 2.7$
Jets	$p_T > 30$ GeV, $\|y\| < 4.4$
Lepton selection and pairing	
Lepton kinematics	$p_T > 20, 15, 10$ GeV
Leading pair (m_{12})	SFOC lepton pair with smallest $\|m_Z - m_{\ell\ell}\|$
Subleading pair (m_{34})	remaining SFOC lepton pair with smallest $\|m_Z - m_{\ell\ell}\|$
Event selection (at most one quadruplet per event)	
Mass requirements	50 GeV$< m_{12} <$ 106 GeV and 12 GeV $< m_{34} <$ 115 GeV
Lepton separation	$\Delta R(\ell_i, \ell_j) > 0.1$
Lepton/Jet separation	$\Delta R(\ell_i, \text{jet}) > 0.1$
J/ψ veto	$m(\ell_i, \ell_j) > 5$ GeV for all SFOC lepton pairs
Mass window	105 GeV $< m_{4\ell} <$ 160 GeV
If extra lepton with $p_T > 12$ GeV	Quadruplet with largest matrix element value

Fiducial region as close as possible to analysis event selection. Almost no extrapolation with ≈ 50% efficiency.

$H \rightarrow ZZ$ fid/diff cross section results

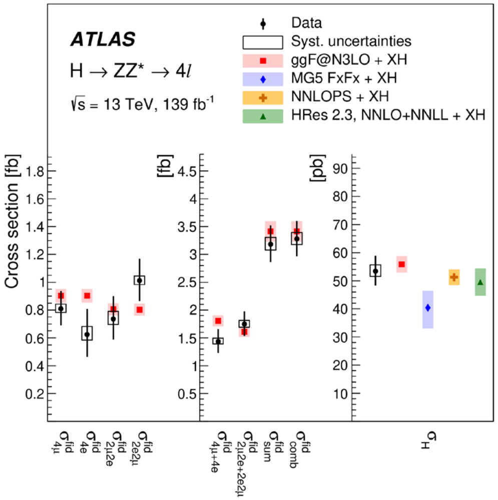

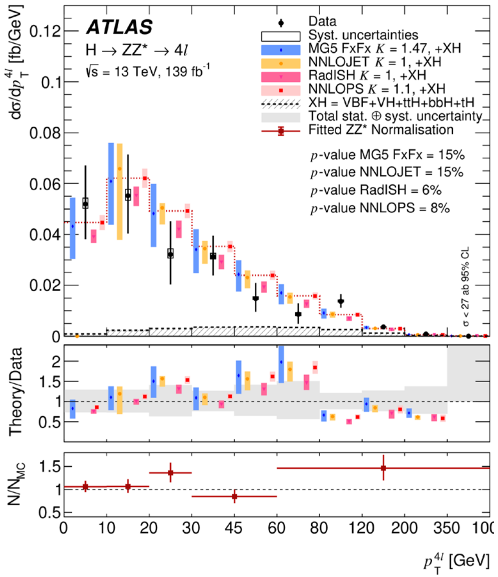

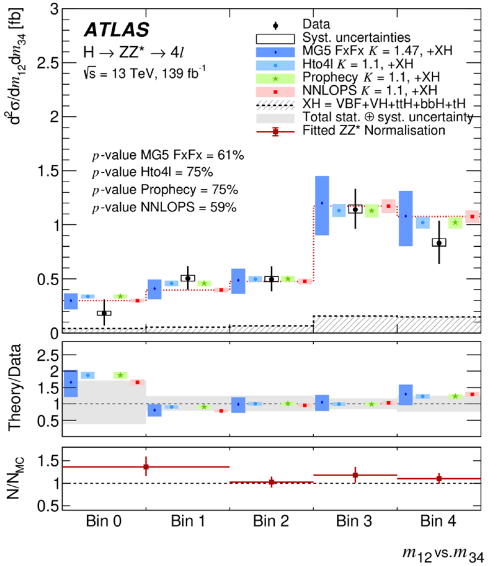

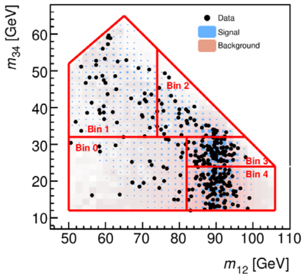

20 different 1D and 2D differential cross sections are measured!

$H \to ZZ$ STXS interpretation

- $H \to ZZ$ events are used to perform STXS measurement using the Stage-1.1 framework.
- Events are categorized based on the number of additional leptons, b-jets, $p_T^{4\ell}$, and on the overall number of jets.
- Inside each category, a NN (both simple MLPs and RNNs) is used to discriminate different production modes and background.
- These NN have either two or three output neurons depending on whether the region receive important contributions from more than one production mode.

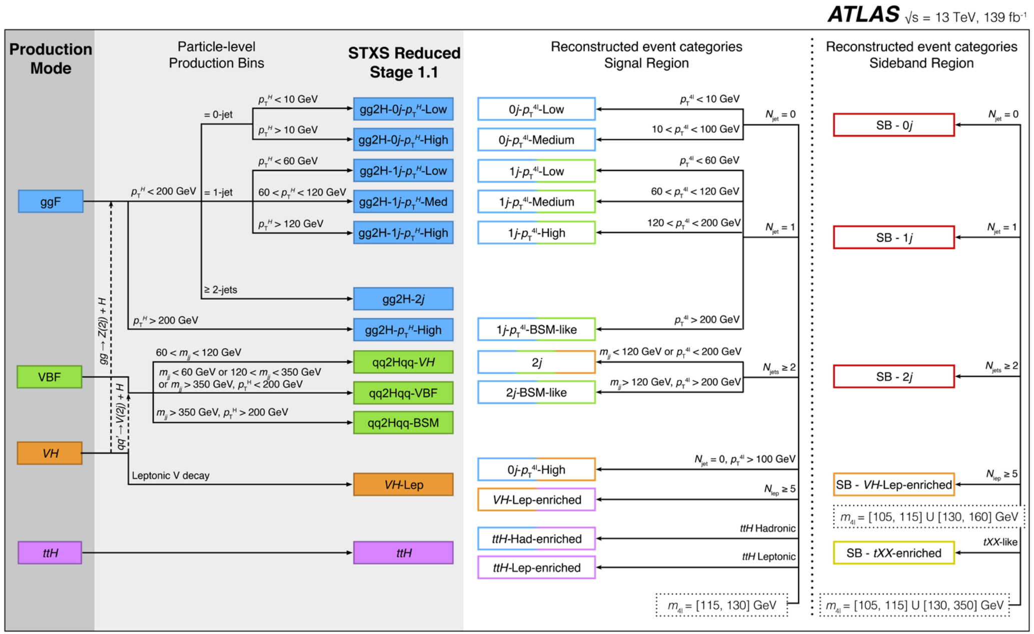

$H \to ZZ$ STXS interpretation

- $H \to ZZ$ events are used to perform STXS measurement using the Stage-1.1 framework.
- Events are categorized based on the number of additional leptons, b-jets, $p_T^{4\ell}$, and on the overall number of jets.
- Inside each category, a NN (both simple MLPs and RNNs) is used to discriminate different production modes and background.
- These NN have either two or three output neurons depending on whether the region receive important contributions from more than one production mode.

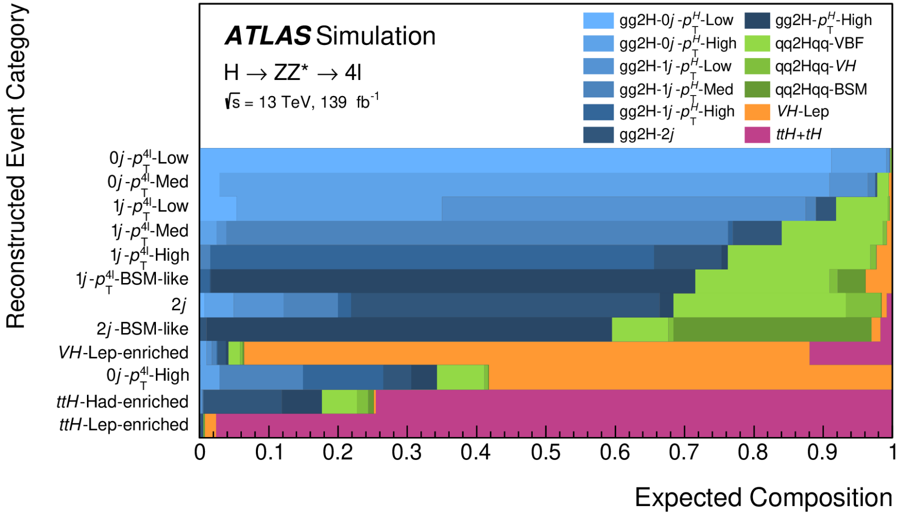

$H \to ZZ$ STXS results

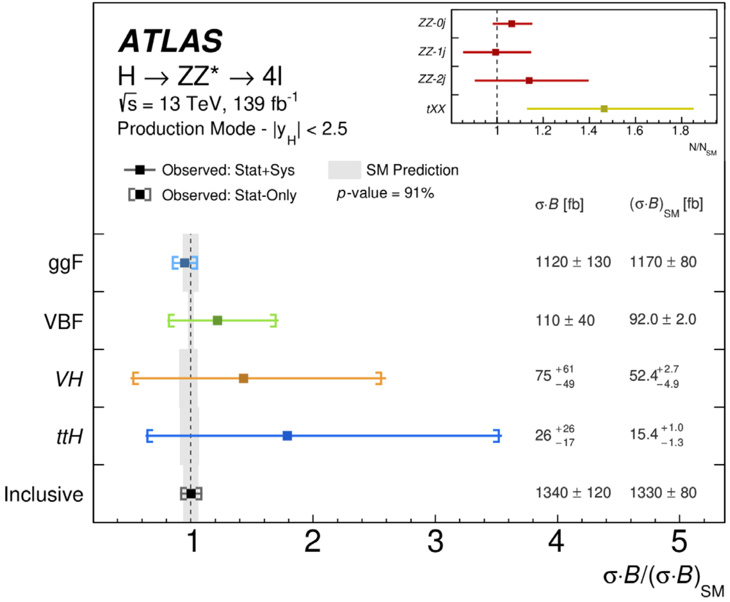

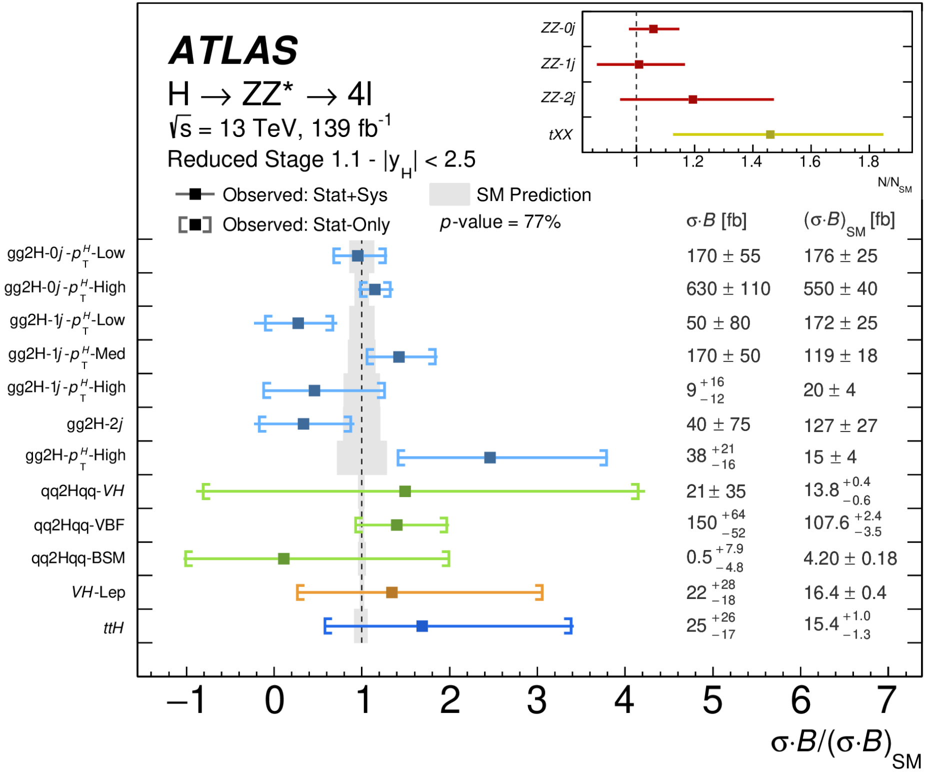

ATLAS EXPERIMENT

UMassAmherst

$H \to ZZ$ STXS results

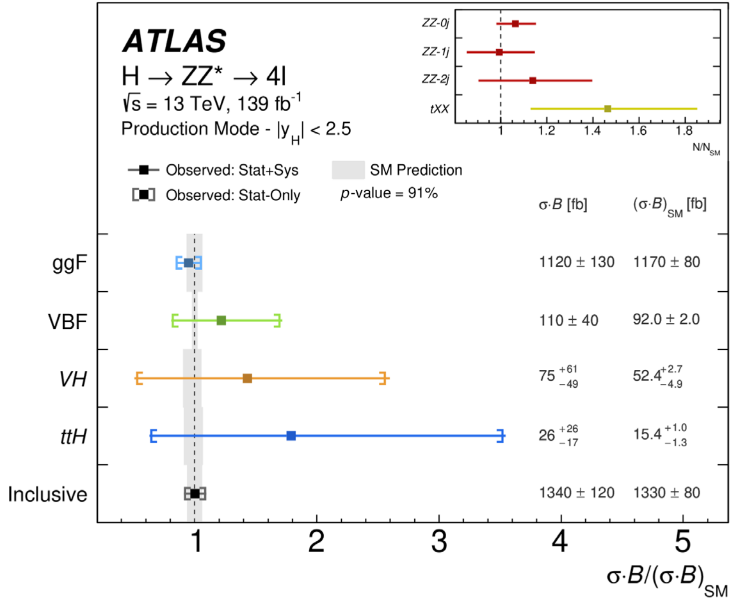

“BSM” bins

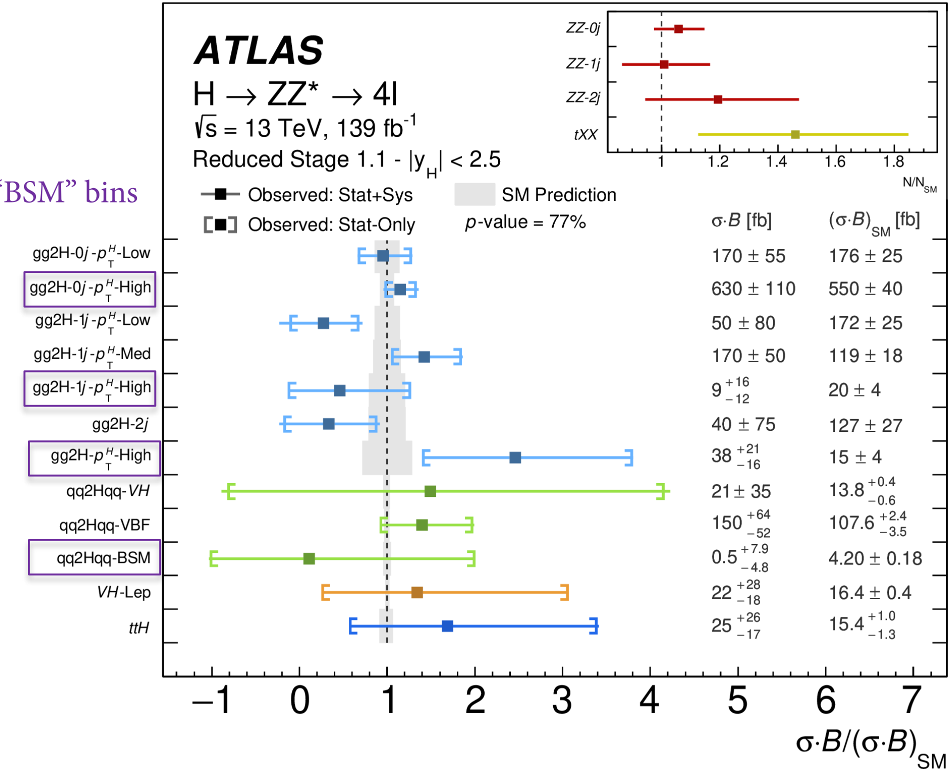

$H \rightarrow ZZ$ EFT interpretation

- Measurements in the Stage-1.1 STXS categories are used to set limits on dimension-6 EFT operators.
- All limits are expressed in TeV^{-2} units
- For VBF, VH, and $t\bar{t}H$, quadratic contributions (proportional to Λ^{-4}) are included when extracting limits. Dimension-8 operators are not included.

CP-even			CP-odd			Impact on	
Operator	Structure	Coeff.	Operator	Structure	Coeff.	production	decay
O_{uH}	$HH^\dagger \bar{q}_p u_r \tilde{H}$	c_{uH}	O_{uH}	$HH^\dagger \bar{q}_p u_r \tilde{H}$	$c_{\tilde{u}H}$	ttH	-
O_{HG}	$HH^\dagger G^A_{\mu\nu} G^{\mu\nu A}$	c_{HG}	$O_{H\tilde{G}}$	$HH^\dagger \tilde{G}^A_{\mu\nu} G^{\mu\nu A}$	$c_{H\tilde{G}}$	ggF	Yes
O_{HW}	$HH^\dagger W^l_{\mu\nu} W^{\mu\nu l}$	c_{HW}	$O_{H\widetilde{W}}$	$HH^\dagger \widetilde{W}^l_{\mu\nu} W^{\mu\nu l}$	$c_{H\widetilde{W}}$	VBF, VH	Yes
O_{HB}	$HH^\dagger B_{\mu\nu} B^{\mu\nu}$	c_{HB}	$O_{H\tilde{B}}$	$HH^\dagger \widetilde{B}_{\mu\nu} B^{\mu\nu}$	$c_{H\tilde{B}}$	VBF, VH	Yes
O_{HWB}	$HH^\dagger \tau^l W^l_{\mu\nu} B^{\mu\nu}$	c_{HWB}	$O_{H\widetilde{W}B}$	$HH^\dagger \tau^l \widetilde{W}^l_{\mu\nu} B^{\mu\nu}$	$c_{H\widetilde{W}B}$	VBF, VH	Yes

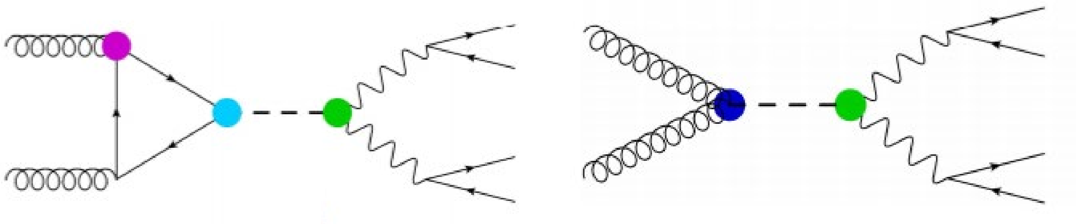

ATLAS EXPERIMENT

UMassAmherst

$H \to ZZ$ EFT interpretation

- Measurements in the Stage-1.1 STXS categories are used to set limits on dimension-6 EFT operators.
- All limits are expressed in TeV^{-2} units
- For VBF, VH, and $t\bar{t}H$, quadratic contributions (proportional to Λ^{-4}) are included when extracting limits. Dimension-8 operators are not included.

CP-even			CP-odd			Impact on	
Operator	Structure	Coeff.	Operator	Structure	Coeff.	production	decay
O_{uH}	$HH^\dagger \bar{q}_p u_r \tilde{H}$	c_{uH}	O_{uH}	$HH^\dagger \bar{q}_p u_r \tilde{H}$	$c_{\tilde{u}H}$	ttH	-
O_{HG}	$HH^\dagger G^A_{\mu\nu} G^{\mu\nu A}$	c_{HG}	$O_{H\tilde{G}}$	$HH^\dagger \tilde{G}^A_{\mu\nu} G^{\mu\nu A}$	$c_{H\tilde{G}}$	ggF	Yes
O_{HW}	$HH^\dagger W^l_{\mu\nu} W^{\mu\nu l}$	c_{HW}	$O_{H\tilde{W}}$	$HH^\dagger \tilde{W}^l_{\mu\nu} W^{\mu\nu l}$	$c_{H\tilde{W}}$	VBF, VH	Yes
O_{HB}	$HH^\dagger B_{\mu\nu} B^{\mu\nu}$	c_{HB}	$O_{H\tilde{B}}$	$HH^\dagger \tilde{B}_{\mu\nu} B^{\mu\nu}$	$c_{H\tilde{B}}$	VBF, VH	Yes
O_{HWB}	$HH^\dagger \tau^l W^l_{\mu\nu} B^{\mu\nu}$	c_{HWB}	$O_{H\tilde{W}B}$	$HH^\dagger \tau^l \tilde{W}^l_{\mu\nu} B^{\mu\nu}$	$c_{H\tilde{W}B}$	VBF, VH	Yes

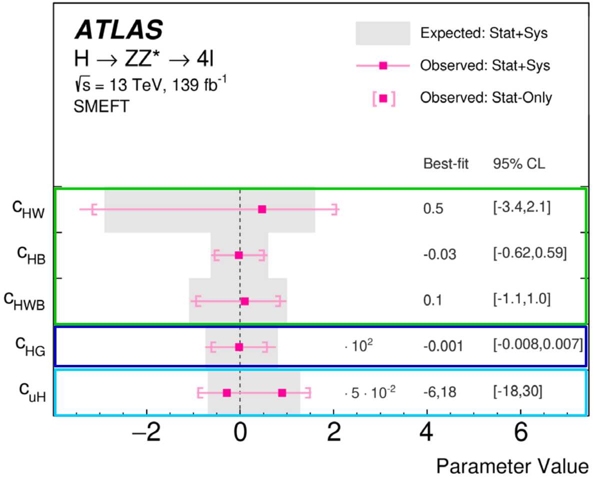

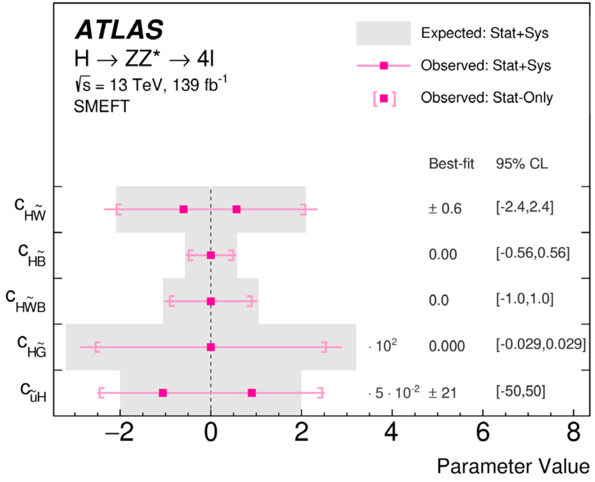

Conclusions

- Higgs boson decays to gauge boson are clean experimental probes for measurements of production and decay properties
- ATLAS has performed several Higgs measurements in the WW, ZZ, and $\gamma\gamma$ final states that go beyond the simple inclusive cross section.
- A large number of fiducial, differential, and simplified template cross sections have been measured.
- These measurements were interpreted as searches for physics beyond the SM in an EFT framework.

UMassAmherst
The Commonwealth's Flagship Campus